CeO_2 Nanoplates

DOI: 10.1002/anie.201101043

Synthesis and Oxygen Storage Capacity of Two-Dimensional Ceria Nanocrystals**

*Dianyuan Wang, Yijin Kang, Vicky Doan-Nguyen, Jun Chen, Rainer Küngas, Noah L. Wieder, Kevin Bakhmutsky, Raymond J. Gorte, and Christopher B. Murray**

Shape-controlled synthesis of inorganic nanomaterials has received great attention[1–9] due to their unique shape-dependent properties and their various applications in catalysis,[1,10,11] electronics,[6,12] magnetics,[7,12] optics,[13] and biomedicine.[14] Among these nanomaterials, ultrathin two-dimensional (2D) anisotropic nanomaterials are especially attractive due to their high surface-to-volume ratio and potential quantum size effects.[15,16] A variety of approaches have been developed to prepare such nanomaterials. Typical methods include vapor deposition,[17] templated synthesis,[18] electrochemical deposition,[19] sol–gel processing,[20] and solvothermal/hydrothermal treatments.[21] Solution-phase chemical synthesis has proven particularly effective in controlling the size and morphology of the nanomaterials.[1,2,6–8,10,16,22]

Ceria has been widely used in catalysis,[23–30] optics,[31] sensors,[32] and solid oxide fuel cells.[33] Due to its high oxygen storage capacity (OSC), which originates from easy conversion between CeO_2 and CeO_{2-x}, ceria has found its primary utilization in catalysis as an oxygen carrier.[23,30,34–37] Ceria nanomaterials with various morphologies, mainly polyhedra, have been reported.[5,16,20,21,38] Recently, 1D ceria nanostructures, such as nanowires, have also been reported.[20] However, with the exception of one report on the preparation of nanosheets,[16] well-controlled 2D ceria nanomaterials have not been explored and the comparison of the OSC properties between 3D and 2D structures has not been possible. On the other hand, the different properties of the (100), (110), and (111) ceria facets has been debated.[5,28,39] There is no consensus on whether crystallographic orientation or particle size affects reactivities.[40] Therefore, high-quality ceria nanocrystals selectively exposing different low Miller-index surfaces, are crucial to enabling experiments that resolve the controversy.

Here we report a simple, robust solution-phase synthesis of ultrathin ceria nanoplates in the presence of mineralizers.[41] The morphology of nanoplates can be easily controlled by changing reaction parameters, such as precursor ratio, reaction time, etc. In addition, we also prepare ceria nanomaterials in various 3D morphologies by hydrothermal[21] and combustion[42] methods. The OSC of our 2D ceria materials have been tested and compared to the OSC of their 3D counterparts.

In brief, the synthesis of ceria nanoplates involves the thermal decomposition of cerium acetate at 320–330 °C in the presence of oleic acid and oleylamine as stabilizers and employs sodium diphosphate or sodium oleate as mineralizers. Transmission electron microscopy (TEM) images of ceria nanoplates are shown in Figure 1. Square ceria nanoplates (S-nanoplates, Figure 1a) with an edge length of 11.9 nm ($\sigma = 7\%$), are synthesized with sodium diphosphate as the mineralizer while elongated ceria nanoplates (L-nanoplates, Figure 1e) with a length of 151.6 nm ($\sigma = 9\%$) and a width of 14.3 nm ($\sigma = 12\%$), are produced with sodium oleate as the mineralizer. The nanoplates in both samples have a thickness of about 2 nm. As shown in Figure 1c and g, the stacks of nanoplates confirm that the sample consists of 2D plates rather than 3D cubes or rods. S-nanoplates readily form the demonstrated stacking arrays as seen in drop-cast TEM samples. L-nanoplates only form stacks by a self-assembly at a liquid–liquid (e.g. hexane–ethylene glycol) interface.[43] The S-nanoplates also self-assemble to a ceria nanosheet at a hexane–acetonitrile interface, as shown in Figure 3a. High-resolution TEM (HRTEM) images of both nanoplates (Figures 1d,h and S1c in the Supporting Information) reveal an interplanar distance of 0.27 nm, consistent with the (200) lattice spacing of the ceria crystal. The fast Fourier transform (FFT) patterns confirm the {100} textures of ceria nanoplates. Plates (e.g. square plates) could be enclosed by either six (100) facets or a combination of two (100) facets and four (110) facets. As illustrated in Figure S1, our HRTEM images and simulations of HRTEM images suggest that our ceria nanoplates are enclosed by six (100)

[*] D. Y. Wang,[+] Y. J. Kang,[+] Prof. C. B. Murray
Department of Chemistry
University of Pennsylvania, Philadelphia, PA 19104 (USA)
E-mail: cbmurray@sas.upenn.edu
V. Doan-Nguyen, J. Chen, Prof. C. B. Murray
Department of Materials Science and Engineering
University of Pennsylvania, Philadelphia, PA 19104 (USA)
D. Y. Wang[+]
College of Science, Jiujiang University
Jiujiang 332005 (P.R. China)
R. Küngas, N. L. Wieder, K. Bakhmutsky, Prof. R. J. Gorte
Department of Chemical and Biomolecular Engineering
University of Pennsylvania, Philadelphia, PA 19104 (USA)
[+] These authors contributed equally to this work.

[**] The following institutions are acknowledged for support: National Natural Science Foundation of China (No. 51062008) (to D.Y.W.), the Nano/Bio Interface Center through the National Science Foundation NSEC DMR08-32802 (to Y.J.K. and V.D.-N., for function testing of nanocatalysts), the U.S. Army Research Office (ARO) under award number MURI W911NF-08-1-0364 (to Y.J.K. and J.C.), and the Department of Energy, Office of Basic Energy Sciences, Chemical Sciences, Geosciences and Biosciences Division, Grant DE-FG02-85ER13350 (to R.K., N.L.W., K.B., R.J.G.). C.B.M. thanks the Richard Perry University Professorship for the support of his supervisor role.

Supporting information for this article is available on the WWW under http://dx.doi.org/10.1002/anie.201101043.

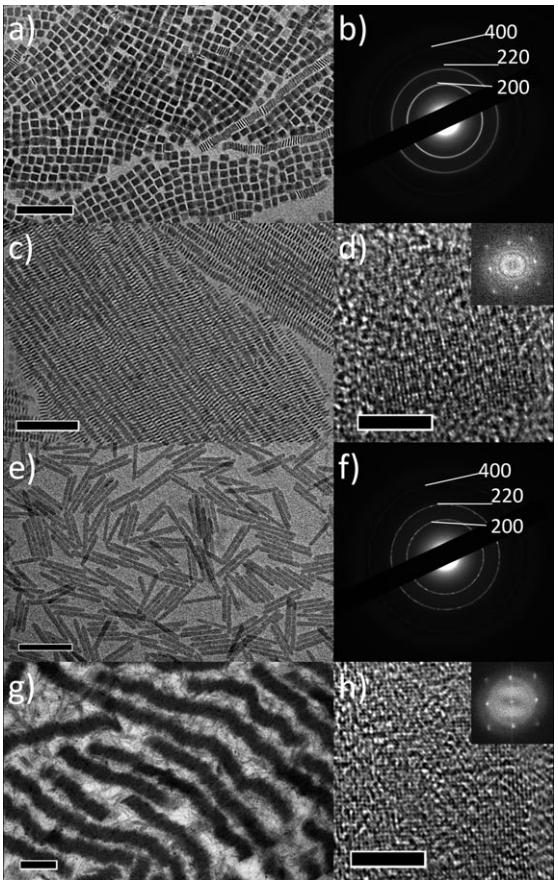

Figure 1. TEM images of a) square ceria nanoplates, c) stacking square ceria nanoplates, e) elongated ceria nanoplates, and d) stacking elongated ceria nanoplates; SAED patterns of b) square ceria nanoplates and f) elongated ceria nanoplates; HRTEM images of d) square ceria nanoplates and h) elongated ceria nanoplates. Insets of (d) and (h): FFT patterns of HRTEM images. Scale bars: a,c) 100 nm, e,g) 200 nm, d,h) 5 nm.

facets, similar to reported gadolinium oxide nanoplates.[22] Selected area electron diffraction (SAED) patterns of ceria nanoplates (Figure 1 b,f) show the enhanced (200), (220) and (400) diffraction rings, consistent to the proposed plate structures.

The X-ray diffraction (XRD) patterns (Figure 2) of the ceria nanoplates confirm the fluorite crystal structure (JCPDS No. 34-0394). The XRD pattern of S-nanoplates shows diminished (200) and (400) peaks, due to the preferred orientation (stacking) as shown in Figure 1 c. For the L-nanoplates, the sharp (200), (400), and broadened other peaks indicate that the dimension is relatively large on {100} facets but very small on any other facets.

The key to this nanoplate synthesis is the incorporation of mineralizers that accelerate the crystallization process and control the morphology of ceria nanocrystals. In the absence of mineralizers, product yield of ceria nanocrystals is very low, and the morphologies are not controlled, as shown in Figure S2. In the presence of mineralizers, the syntheses are very easy to control (i.e., reaction parameters are acceptable in a large range). The nanoplate synthesis can be done even under the ambient environment (i.e. without inert gas

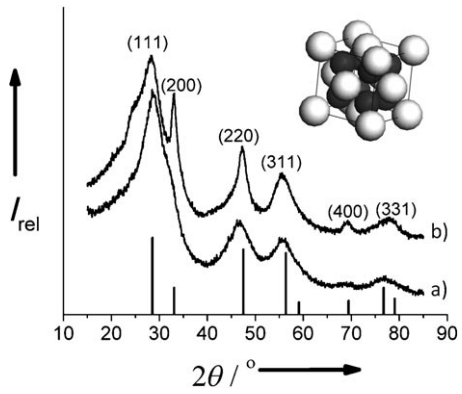

Figure 2. XRD patterns of a) square ceria nanoplates and b) elongated ceria nanoplates. Inset is the unit cell of CeO_2.

protection) in the presence of mineralizers. The stabilizer/solvent combination allows a high reaction temperature (above 320 °C) which is required to form nanoplates. The shape and size of ceria nanoplates can be also controlled by adjusting the synthesis parameters such as the ratio of the stabilizers and the reaction time. For example, increasing the amount of stabilizers (i.e. oleic acid and oleylamine) but keeping other conditions identical to the synthesis of S-nanoplates, circular ceria nanoplates with a diameter of 12 nm ($\sigma = 6\,\%$) are produced (Figure 3 b); the L-nanoplates with a

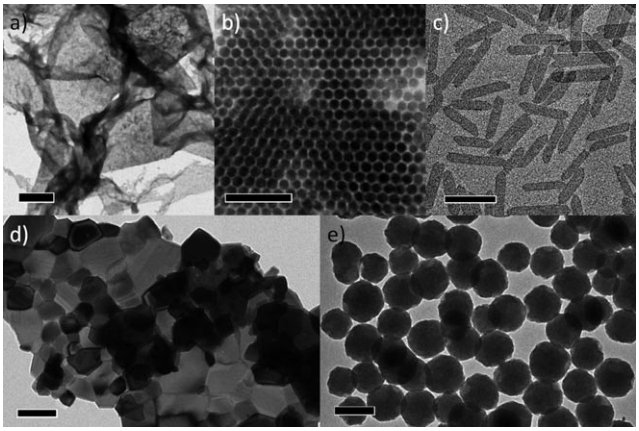

Figure 3. TEM images of a) nanosheets self-assembled from square ceria nanoplates, b) round ceria nanoplates, c) less elongated ceria nanoplates, d) ceria nanomaterials prepared by combustion, and e) hydrothermally synthesized ceria nanospheres. Scale bars: a) 1 μm, b–e) 100 nm.

reduced length (80–120 nm) are made by decreasing the reaction time (Figure 3 c).

For a performance comparison of OSC, ceria nanomaterials and ceria nanospheres were also prepared by the combustion method[42] (Figure 3 d) and the hydrothermal method[21] (Figure 3 e). The typical OSC measurements involve gas-phase reactions in pulse mode (flow titration),[5,44] and gas chromotography or mass spectrometry for detection. These OSC measurements usually require relatively complicated experimental setups. Here, we introduce a simple OSC

measurement technique using cyclic thermogravimetric analysis (TGA). In brief, oxygen gas and reductive hydrogen gas are alternately introduced into a commerical TGA system (e.g. TA Instruments, SDT Q600 TGA/DSC), the mass changes of the ceria samples are then measured and converted to OSC.[45,46]

The OSC measurements were carried out at 300 °C. For pre-treatment, each ceria sample is heated in an oxygen-rich environment to remove the organic stablizers and subsequently heated in 5 % hydrogen (Ar balance) to reduce the surface. The mass change in response to alternating oxidative and reducing environments indicates the cycles of oxygen uptake and release (Figure 4a). The TGA data are averaged

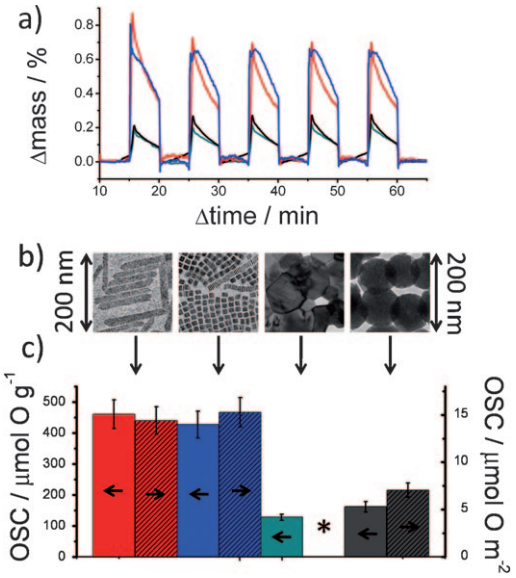

Figure 4. a) TGA data showing the periodical mass change of ceria nanomaterials when O_2 and H_2 are alternately introduced. b) TEM images and c) OSC of ceria nanomaterials. Color code: red, elongated ceria nanoplates; blue, square ceria nanoplates; green, combustion prepared ceria nanomaterials; black, hydrothermally synthesized ceria spheres. * surface area of combustion-prepared ceria is too small to make this comparison.

and then are converted to OSC, as shown in Figure 4c. The L-nanoplates exhibit the highest OSC of 461 μmol O g^{-1}, almost triple that of the ceria nanospheres synthesized by the hydrothermal method (162 μmol O g^{-1}) and approximately four times that of combustion-prepared ceria nanomaterials (128 μmol O g^{-1}). For the S-nanoplates, the reduced OSC of 427 μmol O g^{-1} is ascribed to the stacking of nanoplates, which leads to a reduction in the accessible surface area of ceria nanoplates. Previous studies have reported that the surface reactivity is higher on the (100) surface of ceria than on either (110) or (111),[39] and the energy required to form oxygen vacancies is less on (100) and (110) than that on (111).[47] Therefore, these earlier research results predict that exposure of more {100} planes should facilitate the formation of oxygen vacancies, thus, enhancing the OSC of ceria materials. Our ceria nanoplates are enclosed by (100) facets, allowing us to test this prediction.

The measured surface area of ceria nanoplates is 28 $m^2 g^{-1}$ for S-nanoplates and 32 $m^2 g^{-1}$ for L-nanoplates. These surface areas are lower than reported ceria nanomaterials,[5,21] and maybe the result of significant aggregation (Figure S5) due to the plate morphology. The S-nanoplates should have higher surface area; however, they actually show a lower surface area than L-nanoplates. This confirms that the aggregation causes the reduction in surface area, due to the S-nanoplates being able to more easily stack than L-nanoplates as described earlier (Figure 1). The surface-area-normalized OSC for ceria spheres is 7.0 μmol O m^{-2}, which is close to the theoretical OSC of ceria surfaces [5.7 μmol O m^{-2} for (100) and 6.6 μmol O m^{-2} for (111)],[5] indicating that the oxygen storage at 300 °C is restricted to surface for the ceria spheres prepared by hydrothermal treatment. In contrast, the surface-area-normalized OSC for ceria nanoplates (15.3 μmol O m^{-2} for S-nanoplates and 14.4 μmol O m^{-2} for L-nanoplates) implies that the oxygen storage is not limited to the surface of the 2D ceria nanocrystals, even at temperature as low as 300 °C. Because the oxygen adsorption first occurs on the surface, the surface-area-to-volume (SA/V) ratio is an important parameter of an oxygen storage material. Regardless of the roughness of surface, the SA/V ratio of the S-nanoplates, L-nanoplates, and nanospheres are calculated to be 1.33, 1.16, and 0.066 nm^{-1}, respectively. The combustion-prepared ceria materials have an even lower SA/V ratio due to their large grain size. Therefore, with the high theoretical value of SA/V ratio, the OSC and related catalytic performance of ceria nanoplates have much room to be optimized.

In summary, we have developed a facile, robust synthetic method to prepare 2D ceria nanoplates, which have high theoretical surface-area-to-volume ratio and desirable (100) surfaces. For these reasons, the ceria nanoplates exhibit much higher OSC than the 3D ceria nanomaterials prepared by combustion and hydrothermal methods. With these superior properties, our ceria nanoplates are also promising for many other catalytic applications.

Experimental Section

Synthesis of ceria nanoplates: For square nanoplates, 0.1 g cerium acetate hydrate, 0.53 g sodium diphosphate, 1 mL oleic acid, 2.5 mL oleylamine, and 4.5 mL 1-octadecene are used as starting materials. For elongated nanoplates, the starting materials are 0.1 g cerium acetate hydrate, 0.61 g sodium oleate, 0.5 mL oleic acid, 2 mL oleylamine, and 5.5 mL 1-octadecene. The respective starting materials are mixed well in a three-necked flask at room temperature. The resulting mixture is heated to 120 °C while stirring, and aged at this temperature for 20 min under N_2 atmosphere. The mixture is then heated to 320–330 °C with vigorous magnetic stirring and maintained at this temperature for 30 min under N_2 atmosphere. After 30 min, the solution is cooled down and the ceria nanoplates are flocculated by adding ethanol and centrifugation. The nanoplates are redispersed in hexane.

Characterization and OSC measurement: TEM images and SAED patterns are taken on JEOL1400 operating at 120 kV. HRTEM images are taken on JEOL2010F (200 kV). X-ray diffraction (XRD patterns are obtained on Rigaku Smartlab diffractometer with $Cu_{K\alpha}$ radiation ($\lambda = 1.5418$ Å). The OSC measurements are carried out on TA Instruments, SDT Q600 TGA/DSC.

Received: February 10, 2011
Published online: April 7, 2011

Keywords: ceria · morphology control · nanoplates · nanostructures · oxygen storage

[1] Y. J. Kang, C. B. Murray, *J. Am. Chem. Soc.* **2010**, *132*, 7568.
[2] Y. J. Kang, X. C. Ye, C. B. Murray, *Angew. Chem.* **2010**, *122*, 6292; *Angew. Chem. Int. Ed.* **2010**, *49*, 6156.
[3] Y. J. Xiong, Y. N. Xia, *Adv. Mater.* **2007**, *19*, 3385.
[4] Y. G. Sun, Y. N. Xia, *Science* **2002**, *298*, 2176.
[5] H. X. Mai, L. D. Sun, Y. W. Zhang, R. Si, W. Feng, H. P. Zhang, H. C. Liu, C. H. Yan, *J. Phys. Chem. B* **2005**, *109*, 24380.
[6] X. G. Peng, L. Manna, W. D. Yang, J. Wickham, E. Scher, A. Kadavanich, A. P. Alivisatos, *Nature* **2000**, *404*, 59.
[7] V. F. Puntes, K. M. Krishnan, A. P. Alivisatos, *Science* **2001**, *291*, 2115.
[8] R. Si, Y. W. Zhang, L. P. You, C. H. Yan, *Angew. Chem.* **2005**, *117*, 3320; *Angew. Chem. Int. Ed.* **2005**, *44*, 3256.
[9] S. H. Sun, C. B. Murray, D. Weller, L. Folks, A. Moser, *Science* **2000**, *287*, 1989.
[10] B. Lim, M. J. Jiang, P. H. C. Camargo, E. C. Cho, J. Tao, X. M. Lu, Y. M. Zhu, Y. N. Xia, *Science* **2009**, *324*, 1302.
[11] C. Wang, H. Daimon, T. Onodera, T. Koda, S. H. Sun, *Angew. Chem.* **2008**, *120*, 3644; *Angew. Chem. Int. Ed.* **2008**, *47*, 3588.
[12] F. X. Redl, K. S. Cho, C. B. Murray, S. O'Brien, *Nature* **2003**, *423*, 968.
[13] A. Tao, P. Sinsermsuksakul, P. Yang, *Nat. Nanotechnol.* **2007**, *2*, 435.
[14] M. S. Yavuz, Y. Y. Cheng, J. Y. Chen, C. M. Cobley, Q. Zhang, M. Rycenga, J. W. Xie, C. Kim, K. H. Song, A. G. Schwartz, L. H. V. Wang, Y. N. Xia, *Nat. Mater.* **2009**, *8*, 935.
[15] M. Choi, K. Na, J. Kim, Y. Sakamoto, O. Terasaki, R. Ryoo, *Nature* **2009**, *461*, 246.
[16] T. Yu, B. Lim, Y. N. Xia, *Angew. Chem.* **2010**, *122*, 4586; *Angew. Chem. Int. Ed.* **2010**, *49*, 4484.
[17] X. D. Wang, C. J. Summers, Z. L. Wang, *Nano Lett.* **2004**, *4*, 423.
[18] C. T. Kresge, M. E. Leonowicz, W. J. Roth, J. C. Vartuli, J. S. Beck, *Nature* **1992**, *359*, 710.
[19] J. L. Zhang, M. B. Vukmirovic, Y. Xu, M. Mavrikakis, R. R. Adzic, *Angew. Chem.* **2005**, *117*, 2170; *Angew. Chem. Int. Ed.* **2005**, *44*, 2132.
[20] T. Y. Yu, J. Joo, Y. I. Park, T. Hyeon, *Angew. Chem.* **2005**, *117*, 7577; *Angew. Chem. Int. Ed.* **2005**, *44*, 7411.
[21] X. Liang, X. Wang, Y. Zhuang, B. Xu, S. M. Kuang, Y. D. Li, *J. Am. Chem. Soc.* **2008**, *130*, 2736.
[22] Y. C. Cao, *J. Am. Chem. Soc.* **2004**, *126*, 7456.
[23] T. Bunluesin, R. J. Gorte, G. W. Graham, *Appl. Catal. B* **1998**, *15*, 107.
[24] H. C. Yao, Y. F. Y. Yao, *J. Catal.* **1984**, *86*, 254.
[25] A. Trovarelli, *Catal. Rev.* **1996**, *38*, 439.
[26] Q. Fu, A. Weber, M. Flytzani-Stephanopoulos, *Catal. Lett.* **2001**, *77*, 87.
[27] Q. Fu, H. Saltsburg, M. Flytzani-Stephanopoulos, *Science* **2003**, *301*, 935.
[28] R. Si, M. Flytzani-Stephanopoulos, *Angew. Chem.* **2008**, *120*, 2926; *Angew. Chem. Int. Ed.* **2008**, *47*, 2884.
[29] M. Cargnello, N. L. Wieder, T. Montini, R. J. Gorte, P. Fornasiero, *J. Am. Chem. Soc.* **2010**, *132*, 1402.
[30] W. C. Chueh, C. Falter, M. Abbott, D. Scipio, P. Furler, S. M. Haile, A. Steinfeld, *Science* **2010**, *330*, 1797.
[31] P. Patsalas, S. Logothetidis, C. Metaxa, *Appl. Phys. Lett.* **2002**, *81*, 466.
[32] P. Jasinski, T. Suzuki, H. U. Anderson, *Sens. Actuators B* **2003**, *95*, 73.
[33] S. D. Park, J. M. Vohs, R. J. Gorte, *Nature* **2000**, *404*, 265.
[34] E. S. Putna, T. Bunluesin, X. L. Fan, R. J. Gorte, J. M. Vohs, R. E. Lakis, T. Egami, *Catal. Today* **1999**, *50*, 343.
[35] L. Yang, O. Kresnawahjuesa, R. J. Gorte, *Catal. Lett.* **2001**, *72*, 33.
[36] R. J. Gorte, S. Zhao, *Catal. Today* **2005**, *104*, 18.
[37] F. Zhang, P. Wang, J. Koberstein, S. Khalid, S. W. Chan, *Surf. Sci.* **2004**, *563*, 74.
[38] F. Zhang, Q. Jin, S. W. Chan, *J. Appl. Phys.* **2004**, *95*, 4319.
[39] D. C. Sayle, S. A. Maicaneanu, G. W. Watson, *J. Am. Chem. Soc.* **2002**, *124*, 11429.
[40] R. J. Gorte, *AIChE J.* **2010**, *56*, 1126.
[41] R. Qin, H. Song, G. Pan, X. Bai, B. Dong, S. Xie, L. Liu, Q. Dai, X. Qu, X. Ren, H. Zhao, *Cryst. Growth Des.* **2009**, *9*, 1750.
[42] Y. P. Fu, C. H. Lin, C. S. Hsu, *J. Alloys Compd.* **2005**, *391*, 110.
[43] A. G. Dong, J. Chen, P. M. Vora, J. M. Kikkawa, C. B. Murray, *Nature* **2010**, *466*, 474.
[44] G. Zhou, J. Hanson, R. J. Gorte, *Appl. Catal. A* **2008**, *335*, 153.
[45] Zhang et al. also reported a similar method very recently.[46]
[46] J. Zhang, H. Kumagai, K. Yamamura, S. Ohara, S. Takami, A. Morikawa, H. Shinjoh, K. Kaneko, T. Adschiri, A. Suda, *Nano Lett.* **2011**, *11*, 361.
[47] J. C. Conesa, *Surf. Sci.* **1995**, *339*, 337.

